

Binding of the Atomic Cations Hydrogen through Argon to Water and Hydrogen Sulfide

Brent Westbrook* Katelyn M. Dreux† Gregory S. Tschumper‡

Joseph S. Francisco§ Ryan C. Fortenberry¶

September 23, 2018

Abstract

Water and hydrogen sulfide will bind with every atomic cation from the first three rows of the periodic table. While some atoms bind more tightly than others, explicitly correlated coupled cluster theory computations show that energy is required to be put into the system in order to dissociate these bonds even for noble gas atoms. The most promising systems have shallow entrance potential energy surfaces (PESs) that lie above deeper wells of a different spin. These wells are shown explicitly for H_2OO^+ , H_2SS^+ , and H_2OS^+ where relaxed PESs of the heavy atom bond lengths indicate that quartet states will cross more deeply-bound doublet states allowing for relatively easy association but much more difficult dissociation. In astrophysical regions that are cold and diffuse, such associations could lead to the formation of novel molecules utilizing water (or H_2S) as the building blocks of more rich subsequent chemistry. Recent work has hypothesized that oxywater (H_2OO) may be an intermediate in the formation of molecular oxygen in comets, and this work supports such a conclusion at least from a molecular cation perspective.

*St. Edward's University, Department of Chemistry, Austin, TX 78704 U.S.A.

†University of Mississippi, Department of Chemistry and Biochemistry, University, MS 38677 U.S.A.

‡University of Mississippi, Department of Chemistry and Biochemistry, University, MS 38677 U.S.A.

§University of Pennsylvania, Department of Earth and Environmental Science Philadelphia, PA 19104 U.S.A.

¶University of Mississippi, Department of Chemistry and Biochemistry, University, MS 38677 U.S.A.
E-Mail: r410@olemiss.edu

1 Introduction

Water is sticky. It remains liquid at room temperature while its ammonia, methane, and hydrogen fluoride counterparts are not. This single property has in many ways made water the most important molecule in the universe, especially from an anthropocentric perspective. Water's strong intermolecular forces allow for solvation and moderate or "Goldilocks" viscosity, both of which are essential for life as we know it, including for us humans. The central atom in water, oxygen, is the third-most abundant element in the universe, and its bonding with the most abundant element, hydrogen, implies that water is likely one of the most abundant molecules in the universe. When cold, water regularly forms ices, and these ices form the coma of comets, constitute the boulders of Titan, incubate complex organic molecules as the nursery of prebiotic chemistry, and cool our drinks. However, water is showing up as a potential driver in other chemistries as varied as the formation of interstellar dust grains that eventually become planets^{1,2} to the provenance of the O₂.³

Water has long-been known for its relatively strong intermolecular interaction with itself, other polar molecules, and salts. The cations of such salts are almost always atomic, and they have a long history of scientific investigation.^{4,5} However, the binding of a single water molecule to various atoms has had little impetus for examination since water is almost always used in liquid form in chemistry. Hydronium (H₃O⁺), a known interstellar molecule in its own right,^{6,7} is a notable exception.^{8–10} Additionally, the binding of water molecules to transition metal atomic cations has been discussed in the literature.¹¹ Another example is the oxywater (H₂OO) isomer of hydrogen peroxide which has been known, at least theoretically, for over 25 years.¹² While this molecule is meta-stable with a weak O–O bond,^{13–15} the cation form has been shown to be more robust with a barrier to hydrogen peroxide cation isomerization to be > 25 kcal/mol.^{16–18} The related H₂SS and H₂SS⁺ molecules have also been shown to have similar behavior.^{19,20} In fact, H₂SS⁺ may possibly form through barrierless association of hydrogen sulfide with the sulfur atomic cation²⁰ or through H₂S⁺ association with neutral atomic sulfur since H₂S⁺ has recently been shown likely to exist in astrophys-

ical regions.²¹ Hence, the question remains as to whether the oxygen analogue has a similar near-barrierless association of water and oxygen atomic cation.

Additionally, the association of water and hydrogen sulfide to other atomic cations smaller than iron is currently unclear. While hydration of alkali metal cations have been analyzed,⁴ most studies then move on to solvating these atoms with increasing numbers of water molecules. The cold interstellar medium (ISM) and the interplanetary medium within our own solar system both have densities several orders of magnitude lower than Earth's atmosphere. As a result, isolated water and hydrogen sulfide molecules can interact with atomic cations freely in the gas phase. This could even include noble gas compounds.²²⁻²⁴ Covalent bonds between oxygen atoms and noble gasses have been shown to exist both theoretically and experimentally²⁵⁻²⁷ indicating that these could be viable interstellar species, as well. Regardless, water has been known in the ISM since 1969,²⁸ and comets are accepted to be composed mostly of water. Hence, water molecules may interact with lone atoms or atomic cations in such environments. Most interesting is the surprising discovery of molecular oxygen where it was previously not modeled to be found: in the coma of comet 67P/Churyumov-Gerasimenko.²⁹ This direct *in situ* observation has led to many questions as to the origins of the O₂. One hypothesis is that binding of oxygen atoms to water molecules in the form of the oxywater molecule may play a role in this formation.³

Consequently, the chemistry of water and its isovalent hydrogen sulfide analogue gives indication of possessing a richer chemistry than previously identified. As a first step in this exploration, these two molecules will be paired with the atomic cations from hydrogen to argon in order to determine whether the resulting complexes are tightly bound and/or likely to persist in cold environments. This quantum chemical analysis will build upon the previous theoretical work on H₂SS⁺²⁰ in order to give a broader picture as to the chemistry that can be initiated by H₂O and H₂S.

2 Computational Details

Initial geometries of the various H_2XA^+ complexes, where X=O or S, are obtained using second-order Møller-Plesset perturbation theory (MP2; UMP2 for the open-shell molecules) with the aug-cc-pVDZ basis set for each atom H, He, and B-Ne; aug-cc-pV(D+d)Z for Al-Ar; and cc-pCVDZ for Li, Be, Na, and Mg with Gaussian09.^{30,31} The final computations in this study rely on the explicitly correlated coupled cluster singles, doubles, and perturbative triples, CCSD(T)-F12b, level of theory³²⁻³⁵ within the MOLPRO 2015.1 program.³⁶ The frozen-core approximation is used in all the calculations except those involving lithium and sodium. For the open-shell systems, the UCCSD(T)-F12 method is used. The cc-pVTZ-F12 basis sets are used for the heavy atoms Na-Ar in all computations.^{37,38} The geometry optimizations are followed by harmonic vibrational frequency computations in order to ensure that the structures are minima and to provide zero-point vibrational energies (ZPVEs) in the computation of relative and binding energies. The H_2XA^+ complex binding energies are calculated in two ways: the first assumes that the positive charge is on the atomic cation at the dissociation limit:

$$E_{bind,A^+} = E_{complex} - E_{A^+} - E_{H_2X}, \quad (1)$$

while the second assumes the charge is on the water or hydrogen sulfide:

$$E_{bind,H_2X^+} = E_{complex} - E_A - E_{H_2X^+}. \quad (2)$$

The binding energies computed from the optimized geometries including ZPVE corrections are also computed for the H_2XA^+ complexes with multiple electronic states various spin states in order to produce the most complete set of energies.

Additionally, relaxed CCSD(T)-F12b/cc-pVTZ-F12 scans of the X–A bond at 0.1 Bohr intervals are generated for the four possible molecular cation combinations of water and hydrogen sulfide with atomic oxygen and sulfur. At each point the parameters besides the X–A bond length are allowed to relax. These scans include the lowest-lying $^2\text{A}'$, $^2\text{A}''$, and $^4\text{A}''$ states of H_2SS^+ , H_2OO^+ , H_2OS^+ and H_2SO^+ in a similar

Table 1: Comparison of the Theoretical and Experimental Ionization Potentials (eV).

	MP2/aug-cc-pVDZ	CCSD(T)-F12/cc-pVTZ-F12	Experiment
H	–	13.60	13.59844
Li	5.34	5.39	5.39172
Be	8.05	9.29	9.32263
B	8.04	8.24	8.29803
C	10.82	11.22	11.2603
N	13.93	14.51	14.53414
O	12.06	13.56	13.61806
F	15.77	17.39	17.42282
Ne	19.85	21.57	21.56454
Na	4.95	5.13	5.13908
Mg	6.62	7.53	7.64624
Al	5.60	5.97	5.98577
Si	7.65	8.14	8.15169
P	9.94	10.51	10.48669
S	9.23	10.28	10.36001
Cl	11.83	12.92	12.96764
Ar	14.67	15.76	15.759
H ₂ O	10.90	12.66	12.621
H ₂ S	9.22	10.45	10.453

manner as those from Fortenberry, Trabelsi, and Francisco²⁰ but, again, with geometric relaxation incorporated.

3 Results and Discussion

3.1 Bonding of H₂O and H₂S to Atomic Cations

As an initial calibration, the ionization potentials (IPs, given in Table 1) of every atom as well as water and hydrogen sulfide are compared with experimental data from the NIST database.³⁹ The CCSD(T)-F12/cc-pVTZ-F12 IPs are very close with experiment. The largest difference is for magnesium at 0.11 eV, but most are within 0.05 eV or better compared to experiment. The MP2/aug-cc-pVDZ results underperform and predict IPs that are lower in energy (often by more than 1.0 eV) compared to the explicitly correlated coupled cluster and experimental results. Hence, while the MP2 structures for the bound complexes provide an initial geometry and an estimate for the binding energies, these have been excluded from the remainder of the discussion in order to focus the narrative on the much more trustworthy CCSD(T)-F12 values and

Table 2: The Binding and Relative Energies (kcal/mol) of Water with the Atomic Cations

Complex	Term Symbol	E_{bind,A^+}	E_{bind,H_2O^+}	Relative Energy
H_2OH^+	$^1A'$	-161.49	-139.69	-
H_2OLi^+	1A_1	-32.69	-198.85	-
H_2OBe^+	2A_1	-59.42	-137.04	-
H_2OB^+	1A_1	-48.96	-150.78	-
H_2OC^+	2B_2	-83.87	-117.11	-
H_2ON^+	$^3A''$	-107.94	-65.25	0.0
	1A_1	-82.21	-39.52	25.73
H_2OO^+	$^2A'$	-74.90	-54.08	0.0
	$^2A''$	-63.07	-42.26	11.83
	$^4A''$	-46.84	-26.02	28.06
H_2OF^+	$^1A'$	-150.01	-40.86	-
H_2ONe^+	$^2A'$	-206.44	-0.88	-
H_2ONa^+	1A_1	-21.72	-193.75	-
H_2OMg^+	2A_1	-29.05	-147.30	-
H_2OAl^+	1A_1	-25.54	-179.71	0.0
	3B_2	-54.24	-104.93	74.78
H_2OSi^+	2B_2	-44.99	-149.15	0.0
	4A_2	+41.72	-62.44	86.71
H_2OP^+	$^3A''$	-59.00	-108.61	0.0
	1A_1	-39.22	-88.83	19.77
H_2OS^+	$^2A'$	-34.29	-89.21	0.0
	$^2A''$	-25.85	-80.77	8.44
	$^4A''$	-19.94	-74.86	14.35
H_2OCl^+	$^1A'$	-71.95	-66.00	0.0
	$^3A'$	-38.71	-32.76	33.24
H_2OAr^+	$^2A'$	-77.48	-5.87	-

the implications that they provide. The one exception is for the H_2OHe^+ and H_2SHe^+ complexes where the CCSD(T)-F12 computations could not converge. The MP2 computations indicate that the binding of helium atoms to either water or hydrogen sulfide molecular cations will be on the order of < 0.3 kcal/mol.

3.1.1 Water

The binding energies for water are given in Table 2. The first item for the binding of a hydrogen atomic cation to water is simply another means of stating the proton affinity of water to create hydronium. The literature value for the proton affinity of water is 165 kcal/mol^{5,8,9} which is very close to the magnitude of the ZPVE-corrected binding energy of -161.49 kcal/mol value computed here. The negative value indicates

Table 3: CCSD(T)-F12 Structural Data for the Water Complexes

Complex	Term Symbol	A–O (Å)	O–H (Å)	∠HOA (°)	τ (°)
H_2OH^+	$^1\text{A}'$	0.976	0.976	111.9	126.4
H_2OLi^+	$^1\text{A}_1$	1.829	0.962	127.3	180.0
H_2OBe^+	$^2\text{A}_1$	1.561	0.971	125.2	180.0
H_2OB^+	$^1\text{A}_1$	1.501	0.979	123.4	180.0
H_2OC^+	$^2\text{B}_2$	1.393	0.985	121.8	180.0
H_2ON^+	$^3\text{A}''$	1.451	0.985	111.1	125.3
	$^1\text{A}_1$	1.303	0.993	120.5	180.0
H_2OO^+	$^2\text{A}'$	1.362	0.986	112.3	135.9
	$^2\text{A}''$	1.454	0.992	104.1	112.1
	$^4\text{A}''$	1.968	0.979	103.5	112.2
H_2OF^+	$^1\text{A}'$	1.410	0.992	103.0	115.2
H_2ONe^+	$^2\text{A}'$	2.627	0.999	75.5	114.5
H_2ONa^+	$^1\text{A}_1$	2.252	0.961	127.7	180.0
H_2OMg^+	$^2\text{A}_1$	2.048	0.965	126.9	180.0
H_2OAl^+	$^1\text{A}_1$	2.041	0.968	126.4	180.0
	$^3\text{B}_2$	1.869	0.968	125.2	180.0
H_2OSi^+	$^2\text{B}_2$	1.871	0.970	124.8	180.0
	$^4\text{A}_2$	1.791	0.969	123.7	180.0
H_2OP^+	$^3\text{A}''$	1.835	0.972	119.3	140.8
	$^1\text{A}_1$	1.754	0.973	123.3	180.0
H_2OS^+	$^2\text{A}'$	1.727	0.975	118.6	146.4
	$^2\text{A}''$	1.802	0.979	110.9	119.2
	$^4\text{A}''$	2.367	0.965	122.5	143.6
H_2OCl^+	$^1\text{A}'$	1.734	0.981	109.2	120.3
	$^3\text{A}'$	2.197	0.975	107.0	115.6
H_2OAr^+	$^2\text{A}'$	2.365	0.990	92.24	108.3

that the formation of the complex is favored in our computations. Select geometrical parameters of the optimized, equilibrium form of H_3O^+ are given in Table 3, and the full set of Cartesian geometries (in Å) is given in the supplementary information. The dihedrals are defined as $\tau(\text{H}–\text{X}–\text{A}–\text{H})$. The 0.976 Å bond length and 111.9° bond angle is also in excellent agreement with previous experimental values of 0.976 Å and 111.3°, respectively.⁴⁰ As a result, the computational values for the other molecules should be reliable for predicting the same properties.

To continue, creation or dissociation of H_3O^+ could also proceed through ionization of the water molecule instead of the hydrogen atom. Any association would likely have more water molecular cations than protons since if the two species will react, they will have to be in the same environment and be exposed to the same photons. As such,

the ZPVE-corrected binding is reduced to -139.69 kcal/mol, as given on the top line of Table 2. The reason for the difference lies in the IPs of the two fragments, and, again, these are given in Table 1. The IP of water is computed to be 12.66 eV in close agreement with experiment, while that of a lone H atom is 0.94 eV (or 22.68 kcal/mol) higher in energy. Hence, the reaction would likely favor removal of the hydrogen atom instead of the proton from the water molecule in the gas phase. One consequence of this is the possible charge transfer from free interstellar protons to water molecular cations.

In looking at the overall trends in Table 2, the higher (less negative) of the two numbers for each row has to be assumed to be comparable to the gas phase binding energy since it will be the preferred pathway especially in natural environments like that of comets or protoplanetary disks given that the energy needed for ionization will be lower. Additionally, some atomic cations will have other available spin states. For instance H_2ON^+ has two possible spin states, the $^1\text{A}_1$ and $^3\text{A}''$. Both of these favor ionizing the water over the nitrogen atom upon dissociation demonstrated by the higher binding energies when the charge is on the water molecule. Further analysis of the binding energy reveals that the triplet state requires more energy to break the O–N bond than in the singlet state. Even the noble gases neon and argon show some non-zero binding energies with those from argon being stronger of the two, and the structures of such complexes have a nearly linear $\angle\text{HOH}$ bond angle in H_2OAr^+ that is nearly twice the $\angle\text{HOA}$ value of 92.242° from Table 3. Ionizing the water is much more favorable than the noble gas atoms, but any dissociation from such complexes will be uphill, even if slight in the neon case.

In terms of creating new molecules like the forms of these complexes, however, the most favorable species to interact in the gas phase will have a low-energy, bound excited state where radiative association would not have to take as long.⁴¹ Then, a much more deeply bound second electronic state can be accessed giving an entrance channel followed by a strongly stabilized state. This would preclude further dissociation. H_2SS^+ has been shown to posses such behavior,²⁰ and H_2OO^+ shows similar signs in the $^4\text{A}''$ and $^2\text{A}'$ states, respectively. The $^4\text{A}''$ state minimum lies 26.02 kcal/mol

Table 4: The Binding Energies (kcal/mol) of Hydrogen Sulfide with the Atomic Cations

Complex	Term Symbol	E_{bind,A^+}	E_{bind,H_2S^+}	Relative Energy
H_2SH^+	$^1A'$	-167.78	-94.68	—
H_2SLi^+	$^1A'$	-20.68	-136.70	—
H_2SBe^+	$^2A'$	-46.45	-72.77	—
H_2SB^+	$^1A'$	-38.99	-89.51	—
H_2SC^+	$^2A''$	-87.94	-69.88	—
H_2SN^+	$^3A''$	-140.45	-46.46	0.0
H_2SO^+	1A_1	-134.28	-40.29	6.17
	$^2A'$	-143.46	-71.35	0.0
	$^2A''$	-126.34	-54.22	17.13
H_2SF^+	4A_2	-60.88	+11.23	82.58
	$^1A'$	-241.10	-80.66	0.0
	3B_1	-154.72	+5.72	86.38
H_2SNe^+	$^2A'$	-257.32	-0.46	—
H_2SNa^+	$^1A'$	-13.82	-135.72	—
H_2SMg^+	$^2A'$	-20.48	-87.44	—
H_2SAl^+	$^1A'$	-17.13	-120.00	0.0
H_2SSi^+	$^3A''$	-54.22	-53.61	66.39
	$^2A''$	-41.32	-94.19	—
	$^3A'$	-69.99	-68.30	0.0
H_2SP^+	1A_1	-53.32	-51.63	16.67
	$^2A'$	-63.68	-67.30	0.0
	$^2A''$	-56.50	-60.12	7.18
H_2SS^+	$^4A''$	-29.69	-33.31	33.98
	$^1A'$	-122.54	-65.29	0.0
	$^3A'$	-68.15	-10.90	54.39
H_2SCl^+	3B_1	-56.62	+0.63	65.92
	$^2A'$	-125.40	-2.48	—

below the dissociation limit of H_2O^+ and O, but the $^2A'$ state is even further below at 54.08 kcal/mol. This will be explored more fully in Section 3.2 for both H_2OO^+ and H_2OS^+ . However, the most promising aspect of H_2OO^+ is that the the O–O bond strength is computed here to be more than a third again stronger than a typical peroxide bond. Other potential complexes that could be explored involve the cation forms of water with magnesium, aluminum, silicon, phosphorus, and potentially chlorine. Magnesium and silicon are highly-abundant in the ISM as well as in protoplanetary disks, and such interactions could lead to the formation of protominerals^{2,42} with these cation complexes potentially helping to initiate such processes.

Table 5: CCSD(T)-F12 Structural Data for the Hydrogen Sulfide Complexes Optimized Parameters for F12

Complex	Term Symbol	A–S (Å)	S–H (Å)	∠HSA (°)	τ (°)
H ₂ SH ⁺	¹ A'	1.352	1.352	94.3	94.6
H ₂ SLi ⁺	¹ A'	2.424	1.345	99.8	94.9
H ₂ SBe ⁺	² A'	2.123	1.350	95.6	94.6
H ₂ SB ⁺	¹ A'	2.170	1.351	92.9	94.1
H ₂ SC ⁺	² A''	1.805	1.355	102.7	102.4
H ₂ SN ⁺	³ A''	1.727	1.359	97.6	96.0
	¹ A ₁	1.474	1.369	126.4	180.0
H ₂ SO ⁺	² A'	1.481	1.361	110.0	112.5
	² A''	1.621	1.368	96.6	90.5
	⁴ A ₂	1.547	1.509	84.1	180.0
H ₂ SF ⁺	¹ A'	1.542	1.357	99.1	94.9
	³ B ₁	1.547	1.443	86.9	180.0
H ₂ SNe ⁺	² A'	3.113	1.357	70.7	100.5
H ₂ SNa ⁺	¹ A'	2.801	1.344	100.1	94.7
H ₂ SMg ⁺	² A'	2.669	1.345	98.1	94.6
H ₂ SAl ⁺	¹ A'	2.763	1.345	97.3	94.4
	³ A''	2.303	1.349	106.1	100.5
	² A''	2.350	1.347	102.9	99.2
H ₂ SSi ⁺	³ A''	2.217	1.352	98.9	95.5
	¹ A ₁	1.925	1.356	128.3	180.0
	² A'	2.009	1.353	104.4	101.1
H ₂ SS ⁺	² A''	2.095	1.357	97.7	92.7
	⁴ A''	2.752	1.347	90.8	93.1
	¹ A'	1.978	1.355	99.8	95.3
H ₂ SCl ⁺	³ A'	2.716	1.351	87.7	93.7
	³ B ₁	3.503	1.358	133.4	180.0
	² A'	3.027	1.356	81.6	94.3

3.1.2 Hydrogen Sulfide

The lower IP of H₂S compared to H₂O changes the binding chemistry somewhat, but similar trends are observed for the cation complexes of hydrogen sulfide with the various atoms smaller than argon. The 168.5 kcal/mol proton affinity of H₂S^{5,43} is within 1.0 kcal/mol in magnitude of the -167.78 kcal/mol value computed here and given in Table 4. However and again, the IP of H₂S is less than that of a hydrogen atom indicating that if H₃S⁺ is to form in the ISM, its products would almost certainly be H₂S⁺ and a hydrogen atom which is born out in the E_{bind,A^+} and E_{bind,H_2S^+} energies of Table 4. The structure of H₃S⁺, as well as that of the other complexes for hydrogen sulfide, is given in Table 5.

On the whole, the binding of the various atomic cations to H₂S is weaker than to H₂O. Some such associations, again, could be beneficial for radiative association mechanisms to be fairly fast as long as the binding is not too weak. Additionally, the H₂SS⁺ values computed here match quite closely to those from previous work.²⁰ Furthermore, since the IP of sulfur atoms and H₂S are so similar, dissociation into products with the cation on the molecule or the atom are nearly equally favorable. Other likely complexes that could form from associations of hydrogen sulfide with atomic cations include H₂SO⁺, H₂SMg⁺, H₂SAI⁺, H₂SSi⁺, and H₂SP⁺; nearly all are third-row atom associations.

3.2 Detailed behavior of H₂O and H₂S with O⁺ and S⁺

While the trove of data provided in the previous tables could be picked apart for various applications, the present study will focus on the implications of binding oxygen and sulfur atomic cations in order to compare with the previous H₂SS⁺ study²⁰ and to explore how similar chemistry may proceed for the much more common water molecule and oxygen atoms. Further follow-up on other systems may come in subsequent work.

Figure 1 mirrors the similar potential energy surface (PES) for the S–S stretch in H₂SS⁺ done previously.²⁰ However, the present case allows for the S–H, \angle H–S–S, and τ (H–S–S–H) geometrical parameters to optimize while the chosen S–S bond length is frozen. Even so, the qualitative and most of the quantitative nature of the present curves are in line with the constrained scans from the earlier work. Hence, the behavior of the molecule is predicted to be grossly the same as the S–S bond lengthens. As a result of this, the H₂OO⁺, H₂OS⁺, and H₂SO⁺ structures should be exhibiting the correct minimum and limiting behavior. The states of the constituent pieces given in the caption of Figure 1 will be translatable and consistent for the three other analogues.

The most important item from Figure 1 is that the ⁴A'' state is intercepted nearly at the perfect minimum by the doublet surface as shown in the previous work. This surface splits into the ²A' and ²A'' pieces approaching the minimum. Table 5 has the optimal ⁴A'' S–S bond length at 2.752 Å which is confirmed in the green scan in Figure 1. The ²A' optimized S–S bond length is 2.009 Å which is also consistent with that

Figure 1: The potential energy surface for the S–S bond stretch of H_2SS^+ . The black line is the $^2\text{A}'$ state [${}^1\text{A}_1$ H_2S and $\text{S}^+({}^2\text{D})$], red is $^2\text{A}''$ [${}^1\text{A}_1$ H_2S and orthogonal $\text{S}^+({}^2\text{D})$], and green is $^4\text{A}''$ [${}^1\text{A}_1$ H_2S and $\text{S}^+({}^4\text{S})$].

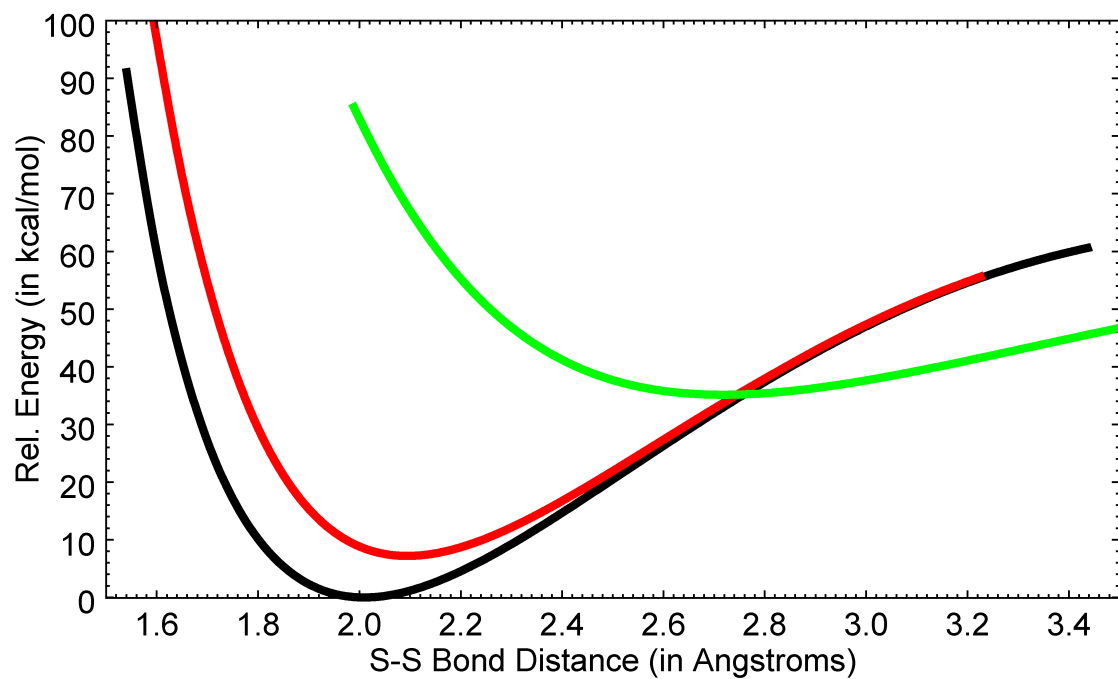
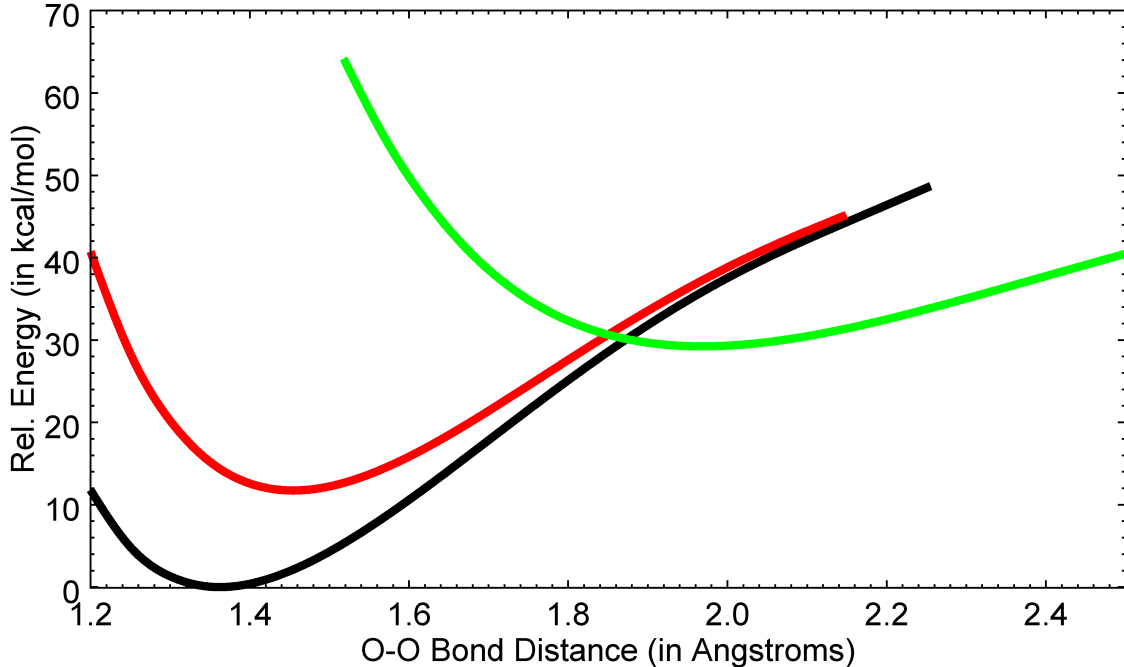


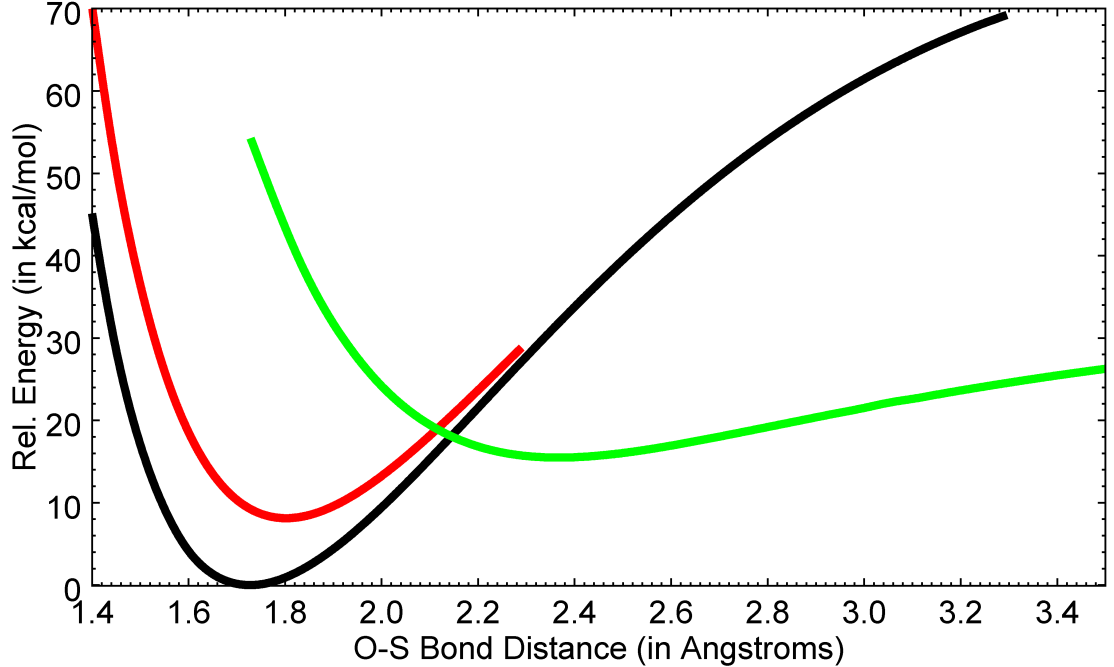
Figure 2: The potential energy surface for the O–O bond stretch of H_2OO^+ . The black line is, again, the $^2\text{A}'$ state, red is $^2\text{A}''$, and green is $^4\text{A}''$.



shown in black. Such an intersection favors spontaneous formation of H_2SS^+ . The reason is that the quartet surface will be accessed at the dissociation limit for the $^1\text{A}_1$ H_2S and $\text{S}^+ ({}^4\text{S})$ components. The quartet surface can have the H_2SS^+ molecule fall down into its well before flipping the spin on one of the electrons in order to move down into the global minimum and remain there. The question remains as to whether the other combinations of S and O will exhibit the same behavior.

Figure 2 is qualitatively the same curve but for H_2OO^+ . The geometries match the minima from Table 3, and the relative energies between states are the same as those in Table 2. While the doublet surface of H_2OO^+ does not fall through the minimum of the quartet surface, the components of the doublet surface both cross the quartet surface not too far away from the minimum. Additionally, the difference in minima between the $^4\text{A}''$ and $^2\text{A}'$ states is only about 30 kcal/mol (only 18 kcal/mol for the $^2\text{A}''$) indicating that such an electronic or vibronic transition is quite possible. As a result, formation of the oxywater cation appears also to be spontaneous, favorable, and

Figure 3: The potential energy surface for the O–S bond stretch of H_2OS^+ . The black line is, again, the $^2\text{A}'$ state, red is $^2\text{A}''$, and green is $^4\text{A}''$.

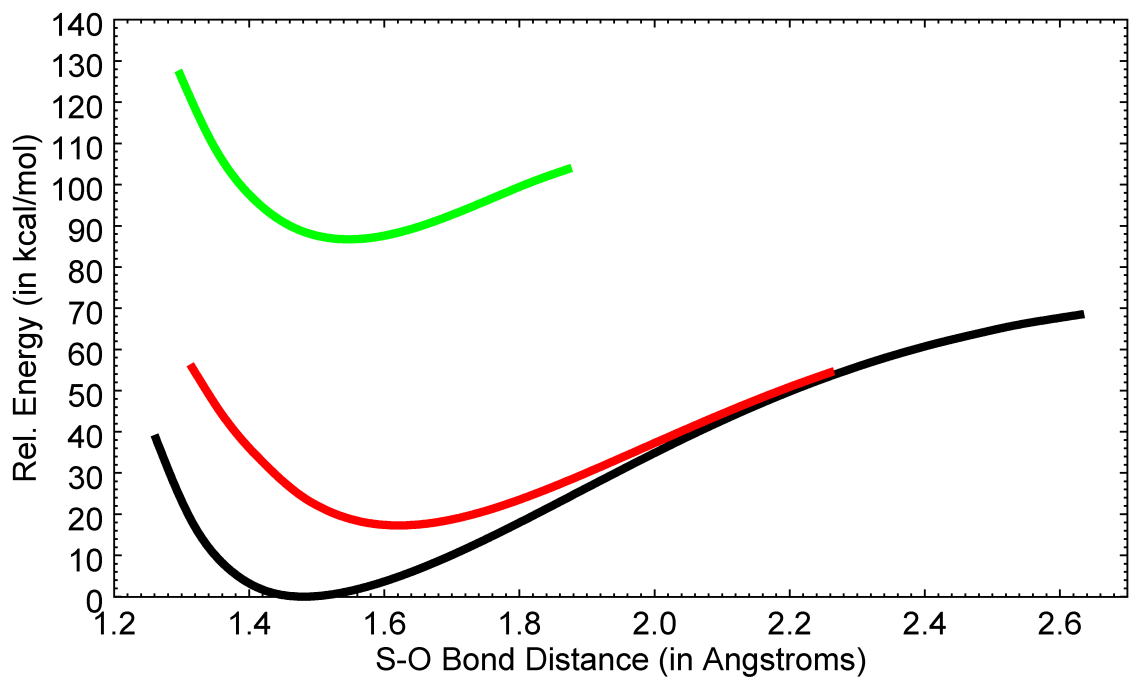


barrierless. Consequently, the oxywater cation should form in regions where both water and atomic oxygen cations are present. Alternatively, if the oxywater neutral forms, photonic ionization will not necessarily dissociate the molecule. Hence, mechanisms for the creation of O–O bonds involving oxywater are supported.

The O–S defined PES scan for H_2OS^+ given in Figure 3 is similar to that for H_2OO^+ . The O–S bond length is longer in the $^4\text{A}''$ state than the point through which the doublet surface passes. However, the difference between the $^4\text{A}''$ minimum and that from the $^2\text{A}'$ state is less than 15 kcal/mol. Additionally, the $^4\text{A}''$ surface is fairly shallow (-19.94 kcal/mol from Table 2) indicating that this complex could form fairly quickly.

The H_2SO^+ S–O PES curve is different from the other three. Figure 4 shows that the $^4\text{A}''$ surface does not cross either component of the doublet surface. Hence, the quartet state will not interact with the doublet state in a favorable way to form H_2SO^+ at least based on the results of this initial study. This form appears to be the exception to

Figure 4: The potential energy surface for the S–O bond stretch of H_2SO^+ . The black line is the $^2\text{A}'$ state, red is $^2\text{A}''$, and green is $^4\text{A}''$.



the rule, but $^2A'$ H_2SO^+ is shown to be stable and can form barrierlessly if the electron spins happen to align in the doublet form at a distance.

4 Conclusions

H_2OO^+ is stable, forms through a barrierless pathway, and is stabilized by a $^2A' \leftarrow ^4A''$ electronic emission from an entrance surface to the global minimum. This indicates that at least the cation form of oxywater is a viable intermediate in reactions where an O–O bond is created. This conclusion follows from the recent work attributing similar properties to the H_2SS^+ analogue.²⁰ The related H_2OS^+ molecular cation also performs in a similar way, but H_2SO^+ does not since the quartet and doublet PESs do not cross. Hence, formation of H_2SO^+ is less likely than the other three. In icy bodies, the oxywater cation is likely to be present if any positive charge is present and could also aid in the formation of molecular oxygen in addition to other proposed mechanisms.³

Furthermore, the associations of water molecules to other atomic cations from hydrogen through argon are also computed. Most notably, the third-row atoms from magnesium even to argon are shown to have favorable binding to both water and hydrogen sulfide. Consequently, in the presence of UV radiation like that from the sun or young stars, water could be a gas phase building block for higher chemistry in comets, protoplanetary disks, and even the ISM where such reactions may not involve solvation, ice, or even liquid chemistry in any way.

5 Acknowledgements

RCF acknowledges funding from start-up monies provided by the University of Mississippi and from NASA APRA Grant NNX17AH15G. Additionally, BW, RCF, and GST acknowledge NSF REU CHE-1460568 grant for support of this work.

References

- [1] Y. Kimura and J. A. Nuth III, *Astrophys. J.*, 2009, **697**, L10–L13.
- [2] M. Komatsu, T. J. Fagan, A. N. Krot, K. Nagashima, M. I. Petaev, M. Kimura and A. Yamaguchi, *Proc. Nat. Acad. Sci. USA*, 2018, **115**, 7497–7502.
- [3] Y. Yao and K. P. Giapis, *Nat. Commun.*, 2017, **8**, 15298.
- [4] E. D. Glendening and D. Feller, *J. Phys. Chem.*, 1995, **99**, 3060–3067.
- [5] E. P. L. Hunter and S. G. Lias, *J. Phys. Chem. Ref. Data*, 1998, **27**, 413–656.
- [6] A. Wootten, F. Boulanger, M. Bogey, F. Combes, P. J. Encrenaz, M. Gerin and L. Ziurys, *Astron. Astrophys.*, 1986, **166**, L15–L18.
- [7] J. M. Hollis, E. B. Churchwell, E. Herbst and F. C. de Lucia, *Nature*, 1986, **322**, 524–526.
- [8] S. M. Collyer and T. B. McMahon, *J. Phys. Chem.*, 1983, **87**, 909–911.
- [9] K. A. Peterson, S. S. Xantheas, D. A. Dixon and T. H. Dunning, Jr., *J. Phys. Chem. A*, 1998, **102**, 2449–2454.
- [10] G. E. Douberty, R. S. Walters, J. Cui, K. D. Jordan and M. A. Duncan, *J. Phys. Chem. A*, 2010, **114**, 4570–4579.
- [11] M. Rosi and C. W. Bauschlicher, Jr., *J. Chem. Phys.*, 1989, **90**, 7264–7272.
- [12] C. Meredith, T. P. Hamilton and H. F. Schaefer III, *J. Phys. Chem.*, 1992, **96**, 9250–9254.
- [13] H. H. Huang, Y. Xie and H. F. Schaefer III, *J. Phys. Chem.*, 1996, **100**, 6076–6080.
- [14] I. I. Moiseev, *J. Mol. Catal. Chem. A*, 1997, **127**, 1–23.
- [15] S. Pehkonen, K. Marushkevich, L. Khriachtchev, M. Räsänen, B. L. Grigorenko and A. V. Nemukhin, *J. Phys. Chem.*, 2007, **111**, 11444–11449.

[16] Y. Xie, W. D. Allen, Y. Yamaguchi and H. F. Schaefer III, *J. Chem. Phys.*, 1996, **104**, 7615–7623.

[17] B. S. Jursic, *J. Molec. Struct.*, 1997, **401**, 45–54.

[18] G. de Petris, A. Cartoni, R. Cipollini and A. Troiani, *Int. J. Mass Spectrom.*, 2006, **249-250**, 311–316.

[19] C. R. Zhou, K. Sendt and B. S. Haynes, *J. Phys. Chem. A*, 2008, **112**, 3239–3247.

[20] R. C. Fortenberry, T. Trabelsi and J. S. Francisco, *J. Phys. Chem. A*, 2018, **122**, 4983–4987.

[21] W. J. Morgan, X. Huang, H. F. Schaefer III and T. J. Lee, *Mon. Not. Royal Astron. Soc.*, 2018.

[22] M. J. Barlow, B. M. Swinyard, P. J. Owen, J. Cernicharo, H. L. Gomez, R. J. Ivison, O. Krause, T. L. Lim, M. Matsuura, S. Miller, G. Olofsson and E. T. Polehampton, *Science*, 2013, **342**, 1343–1345.

[23] P. Schilke, D. A. Neufeld, H. S. P. Müller, C. Comito, E. A. Bergin, D. C. Lis, M. Gerin, J. H. Black, M. Wolfire, N. Indriolo, J. C. Pearson, K. M. Menten, B. Winkel, A. Sánchez-Monge, T. Möller, B. Godard and E. Falgarone, *Astron. Astrophys.*, 2014, **566**, A29.

[24] R. C. Fortenberry, *Int. J. Quant. Chem.*, 2017, **117**, 81–91.

[25] R. A. Theis and R. C. Fortenberry, *Mol. Astrophys.*, 2016, **2**, 18–24.

[26] R. C. Fortenberry and S. R. Gwaltney, *ACS Earth Space Chem.*, 2018, **2**, 491–495.

[27] J. P. Wagner, D. C. McDonald II and M. A. Duncan, *Angew. Chem. Int. Ed.*, 2018, **57**, 5081–5085.

[28] A. C. Cheung, D. M. Rank, C. H. Townes, D. D. Thornton and W. J. Welch, *Nature*, 1969, **221**, 626.

[29] A. Bieler, K. Altwegg, H. Balsiger, A. Bar-Nun, J.-J. Berthelier, P. Bochsler, C. Briois, U. Calmonte, M. Combi, J. D. Keyser, E. F. van Dishoeck, B. Fieth, S. A. Fuselier, S. Gasc, T. I. Gombosi, K. C. Hansen, M. Hässig, A. Jäckel, E. Kopp, A. Korth, L. L. Roy, U. Mall, R. Maggiolo, B. Marty, O. Mousis, T. Owen, H. Rème, M. Rubin, T. Sémon, C.-Y. Tzou, J. H. Waite, C. Walsh and P. Wurz, *Nature*, 2015, **526**, 678–681.

[30] C. Møller and M. S. Plesset, *Phys. Rev.*, 1934, **46**, 618–622.

[31] M. J. Frisch, G. W. Trucks, H. B. Schlegel, G. E. Scuseria, M. A. Robb, J. R. Cheeseman, G. Scalmani, V. Barone, B. Mennucci, G. A. Petersson, H. Nakatsuji, M. Caricato, X. Li, H. P. Hratchian, A. F. Izmaylov, J. Bloino, G. Zheng, J. L. Sonnenberg, M. Hada, M. Ehara, K. Toyota, R. Fukuda, J. Hasegawa, M. Ishida, T. Nakajima, Y. Honda, O. Kitao, H. Nakai, T. Vreven, J. A. Montgomery, Jr., J. E. Peralta, F. Ogliaro, M. Bearpark, J. J. Heyd, E. Brothers, K. N. Kudin, V. N. Staroverov, R. Kobayashi, J. Normand, K. Raghavachari, A. Rendell, J. C. Burant, S. S. Iyengar, J. Tomasi, M. Cossi, N. Rega, J. M. Millam, M. Klene, J. E. Knox, J. B. Cross, V. Bakken, C. Adamo, J. Jaramillo, R. Gomperts, R. E. Stratmann, O. Yazyev, A. J. Austin, R. Cammi, C. Pomelli, J. W. Ochterski, R. L. Martin, K. Morokuma, V. G. Zakrzewski, G. A. Voth, P. Salvador, J. J. Dannenberg, S. Dapprich, A. D. Daniels, O. Farkas, J. B. Foresman, J. V. Ortiz, J. Cioslowski and D. J. Fox, *Gaussian 09 Revision D.01*, 2009, Gaussian Inc. Wallingford CT.

[32] K. Raghavachari, G. W. Trucks., J. A. Pople and M. Head-Gordon, *Chem. Phys. Lett.*, 1989, **157**, 479–483.

[33] T. D. Crawford and H. F. Schaefer III, in *Reviews in Computational Chemistry*, ed. K. B. Lipkowitz and D. B. Boyd, Wiley, New York, 2000, vol. 14, pp. 33–136.

[34] T. B. Adler, G. Knizia and H.-J. Werner, *J. Chem. Phys.*, 2007, **127**, 221106.

[35] G. Knizia, T. B. Adler and H.-J. Werner, *J. Chem. Phys.*, 2009, **130**, 054104.

[36] H.-J. Werner, P. J. Knowles, G. Knizia, F. R. Manby, M. Schütz, P. Celani, W. Györffy, D. Kats, T. Korona, R. Lindh, A. Mitrushenkov, G. Rauhut, K. R.

Shamasundar, T. B. Adler, R. D. Amos, A. Bernhardsson, A. Berning, D. L. Cooper, M. J. O. Deegan, A. J. Dobbyn, F. Eckert, E. Goll, C. Hampel, A. Hesselmann, G. Hetzer, T. Hrenar, G. Jansen, C. Köppl, Y. Liu, A. W. Lloyd, R. A. Mata, A. J. May, S. J. McNicholas, W. Meyer, M. E. Mura, A. Nicklass, D. P. O'Neill, P. Palmieri, D. Peng, K. Pflüger, R. Pitzer, M. Reiher, T. Shiozaki, H. Stoll, A. J. Stone, R. Tarroni, T. Thorsteinsson and M. Wang, *MOLPRO, Version 2015.1, a Package of ab Initio Programs*, 2015, see <http://www.molpro.net>.

[37] T. H. Dunning, K. A. Peterson and A. K. Wilson, *J. Chem. Phys.*, 2001, **114**, 9244–9253.

[38] K. E. Yousaf and K. A. Peterson, *J. Chem. Phys.*, 2008, **129**, 184108.

[39] K. P. Huber, G. Herzberg, J. W. Gallagher and R. D. Johnson, III, in *Constants of Diatomic Molecules*, ed. P. J. Linstrom and W. G. Mallard, National Institute of Standards and Technology, Gaithersburg MD, 20899, 2018, p. 69.

[40] T. J. Sears, P. R. Bunker, P. B. Davies, S. A. Johnson and V. S. Pirk, *J. Chem. Phys.*, 1985, **83**, 2676–2685.

[41] M. Larsson, W. D. Geppert and G. Nyman, *Rep. Prog. Phys.*, 2012, **75**, 066901.

[42] K. A. Kloska and R. C. Fortenberry, *Mon. Not. Royal Astron. Soc.*, 2018, **474**, 2055–2063.

[43] P. Botschwina, A. Zilch, H.-J. Werner, P. Rosmus and E.-A. Reinsch, *J. Chem. Phys.*, 1986, **85**, 5107–5116.